ARMY RESEARCH LABORATORY

Multiscale Modeling of Piezoelectric Materials

by LTC Steven Creighton, Ph.D., Dr. Peter W. Chung, and Dr. John D. Clayton

ARL-TR-4651 **November 2008**

NOTICES

Disclaimers

The findings in this report are not to be construed as an official Department of the Army position unless so designated by other authorized documents.

Citation of manufacturer's or trade names does not constitute an official endorsement or approval of the use thereof.

Destroy this report when it is no longer needed. Do not return it to the originator.

Army Research Laboratory
Aberdeen Proving Ground, MD 21005-5067

ARL-TR-4651 **November 2008**

Multiscale Modeling of Piezoelectric Materials

LTC Steven L. Creighton, Ph.D.
United States Military Academy

Dr. Peter W. Chung
Computational and Information Sciences Directorate, ARL

Dr. John D. Clayton
Weapons and Materials Research Directorate, ARL

REPORT DOCUMENTATION PAGE	Form Approved OMB No. 0704-0188

1. REPORT DATE *(DD-MM-YYYY)*	2. REPORT TYPE	3. DATES COVERED (From - To)
November 2008	Final	October 2007–September 2008

4. TITLE AND SUBTITLE
Multiscale Modeling of Piezoelectric Materials

5a. CONTRACT NUMBER

5b. GRANT NUMBER

5c. PROGRAM ELEMENT NUMBER

6. AUTHOR(S)
LTC Steven L. Creighton, Ph.D.,* Dr. Peter Chung, and Dr. John D. Clayton

5d. PROJECT NUMBER
USMA/ARL

5e. TASK NUMBER

5f. WORK UNIT NUMBER

7. PERFORMING ORGANIZATION NAME(S) AND ADDRESS(ES)
U.S. Army Research Laboratory
ATTN: AMSRD-ARL-CH-HC
Aberdeen Proving Ground, MD 21005-5067

8. PERFORMING ORGANIZATION REPORT NUMBER
ARL-TR-4651

9. SPONSORING/MONITORING AGENCY NAME(S) AND ADDRESS(ES)

10. SPONSOR/MONITOR'S ACRONYM(S)

11. SPONSOR/MONITOR'S REPORT NUMBER(S)

12. DISTRIBUTION/AVAILABILITY STATEMENT
Approved for public release; distribution is unlimited.

13. SUPPLEMENTARY NOTES
*Department of Civil & Mechanical Engineering, United States Military Academy, West Point, NY

14. ABSTRACT
Piezoelectric materials possess tremendous potential in twenty-first century engineering applications. A high-fidelity model is sought that can more accurately predict piezoelectric behavior by embedding parameters typically associated with the fine scale (i.e., atomic scale) into contemporary piezoelectric macroscale formulation. The research presented is theoretical and demonstrates how this can be realized. The material examined is lead-zirconate-titanate. The model presented utilizes an energy potential based on atomistic attractive forces to develop an elastic modulus that is incorporated into classical macroscale piezoelectric governing equations in lieu of the standard elasticity tensor. Also presented will be ideas for future work, whereby the atomistic modulus is utilized in a variational multiscale environment.

15. SUBJECT TERMS
multiscale modeling, piezoelectricity, continuum mechanics, computational science, computational engineering, soldier power

16. SECURITY CLASSIFICATION OF:			17. LIMITATION OF ABSTRACT	18. NUMBER OF PAGES	19a. NAME OF RESPONSIBLE PERSON
a. REPORT	b. ABSTRACT	c. THIS PAGE			Peter W. Chung
UNCLASSIFIED	UNCLASSIFIED	UNCLASSIFIED	UL	24	19b. TELEPHONE NUMBER (*Include area code*) (410) 278-6027

Contents

List of Figures **iv**

1. Introduction **1**

2. PZT Monoclinic Structure **2**

3. Notation **4**

4. Atomistic Behavior and the Constitutive Equation **5**

5. Atomistic Elasticity Tensor **5**

5.1 Atomistic Kinematics 5

5.2 Definition of Potential 6

5.3 Finite Strain and Classical Continuum Mechanics 7

6. Variational Multiscale Formulation **9**

6.1 Multiscale Deformation 10

6.2 Multiscale Kinematics 11

6.3 Multiscale Governing Equations of Solid Mechanics 13

6.4 Governing Equations of Electromagnetism 13

6.5 Variational Equations 14

7. Conclusions and Future Work **14**

7.1 Atomistic Elasticity Tensor 14

7.2 Multiscale Formulation 15

8. References **16**

Distribution List **17**

List of Figures

Figure 1. RPG launcher.....1
Figure 2. Smart controllable rotorcraft twist research. 1
Figure 3. Piezoelectric board inserted into a combat boot.....2
Figure 4. Piezoelectric board. 2
Figure 5. The $PbZr_{0.52}Ti_{0.48}O_3$ (PZT) molecule (Rabe, 2002). 3
Figure 6. Three atoms depicted in the reference and current configurations.....4
Figure 7. Example of multiscale deformation as seen by a piezoelectric board experiencing bending.....10
Figure 8. Some key points made by observing the deformations in a hypothetical thin wire. 11
Figure 9. Multiscale kinematics. Three configurations are used in this framework – reference, intermediate, and current (Creighton et al., 2004). 12

1. Introduction

Piezoelectric materials possess the unique property that when subjected to a deformation, they produce electricity. Conversely, when these materials are subjected to an electric field, they undergo deformation. This unique property has been exploited by researchers and engineers to achieve desired effects such as in the design of the ignition system in the rocket-propelled grenade launcher (RPG) (shown in figure 1); it continues to intrigue researchers with its promise in the design of new systems and devices. New piezoelectric applications are limited only by the imagination. Figure 2 shows rotor blade research conducted at the University of Maryland in an attempt to design smart controllable blades that have desirable twist characteristics.

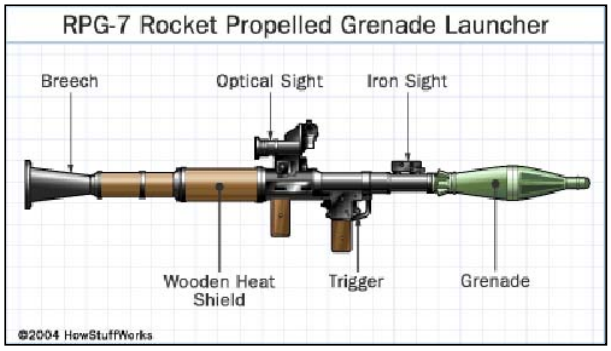

Source: http://science.howstuffworks.com/rpg3.htm.

Figure 1. RPG launcher.

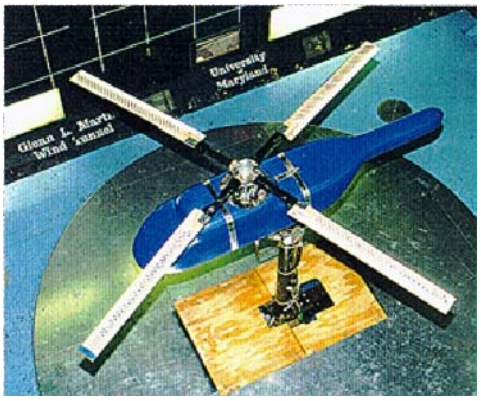

Source: http://www.enae.umd.edu/AGRC/pict/.

Figure 2. Smart controllable rotorcraft twist research.

At the United States Military Academy, students and researchers (Labo, 2005) have researched the incorporation of piezoelectric materials in combat boots (see figures 3 and 4). This research was motivated by an attempt to capture the excess energy generated during the natural gait of a soldier's step. Other uses of piezoelectric materials include sophisticated power generation systems for microsensors and microelectromechanical systems devices and household uses such as ignition switches for propane barbeque grills.

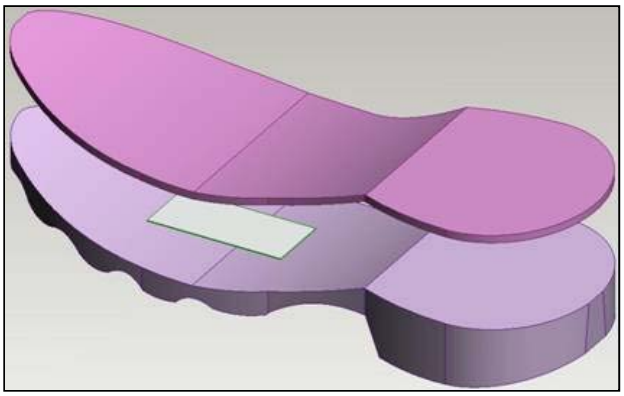

Figure 3. Piezoelectric board inserted into a combat boot.

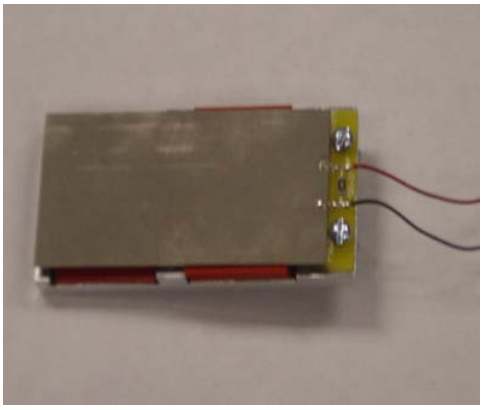

Figure 4. Piezoelectric board.

2. PZT Monoclinic Structure

The introduction to piezoelectric materials just mentioned motivates an explanation of how piezoelectric materials work. To do this, the molecular makeup of these materials must be examined. To limit the scope of this explanation and stay within the context of the available research, the piezoelectric material $PbZr_{0.52}Ti_{0.48}O_3$ will be discussed. The material $PbZr_{0.52}Ti_{0.48}O_3$ (see figure 5) is a subset of piezoelectric materials called PZTs that contain

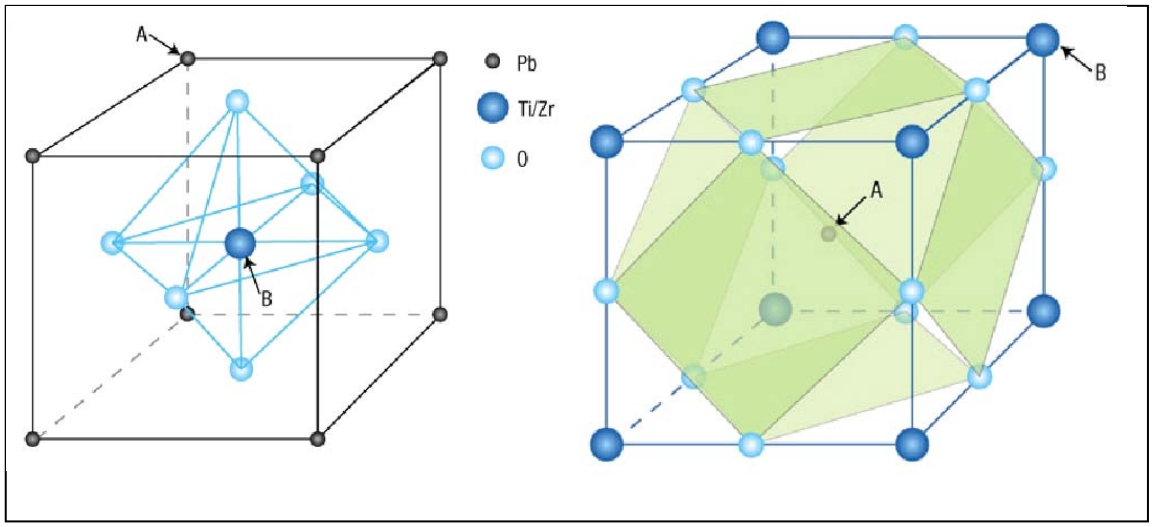

Figure 5. The $PbZr_{0.52}Ti_{0.48}O_3$ (PZT) molecule (Rabe, 2002).

lead (Pb), zirconium (Zr), and titanium (Ti). This material is also a subset of materials called perovskites that are composed of atoms of the ABO_3 form. In $PbZr_{0.52}Ti_{0.48}O_3$, *Pb* is the *A* atom and either *Zr* or *Ti* (randomly distributed) is the *B* atom.

The author of figure 2 (Rabe, 2002) aptly describes this molecule's behavior as follows:

> The ideal perovskite structure (ABO_3) centred on a, the B site (Ti/Zr) and b, the A site (Pb). In the piezoelectric material PZT the Zr and Ti atoms are randomly distributed on the B sites. Using first-principles calculations Grinberg and colleagues[2] show that each Pb atom displaces preferentially towards square green faces with the largest Ti fraction. These local distortions can be correlated with global structure and behaviour. For example, in PZT the displacement of the metal ions (Pb, Ti and Zr) away from the centre of their oxygen cages generates local polarization and ultimately ferroelectricity. c, The net polarization and overall structure of PZT changes with the ratio of Ti:Zr atoms, as shown in the *x*−*T* phase diagram. The six structural phases of PZT at ambient pressure are mostly ferroelectric, with the exception of antiferroelectric behaviour (A) near $PbZrO_3$ and a paraelectric cubic phase (C) at high temperatures. Grinberg *et al*. show that the complex phase behaviour of different Zr/Ti compositions can be explained by averaging the changing distribution of Pb displacements, which depend on their local environment. T = Ti-rich tetragonal phase; R = rhombohedral phase; M = monoclinic ferroelectric phase.

3. Notation

The following portion of this report concerns itself with incorporating the piezoelectric behavior of the PZT molecule shown in figure 5 into a mathematical formulation which can, in turn, be implemented by computational methods. It is appropriate at this point to make clear distinction of the notation used throughout the rest of this report. To discern between scalar and tensoral variables, we will use the standard indicial notation u_i for first-order tensors (i.e., vector variables), u_{ij} for second-order tensors, u_{ikj} for third-order tensors, etc. In a three-dimensional (3-D) calculation, all tensor and vector indices span the range (1, 2, and 3). Variables with no indices will be scalar quantities. Moreover, variables in bold font (e.g., $\mathbf{u}$) will be tensor variables (order implied by usage), and unbold font will imply scalar quantities. When discussing atomistic relationships, atom labels will be denoted by the lone indices i, j, or k in parentheses, usually as superscripts. For example, $\mathbf{r}^{(ij)}$ (or $\mathbf{r}(i, j)$) is the position vector from atom *i* to atom *j* (see figure 6).

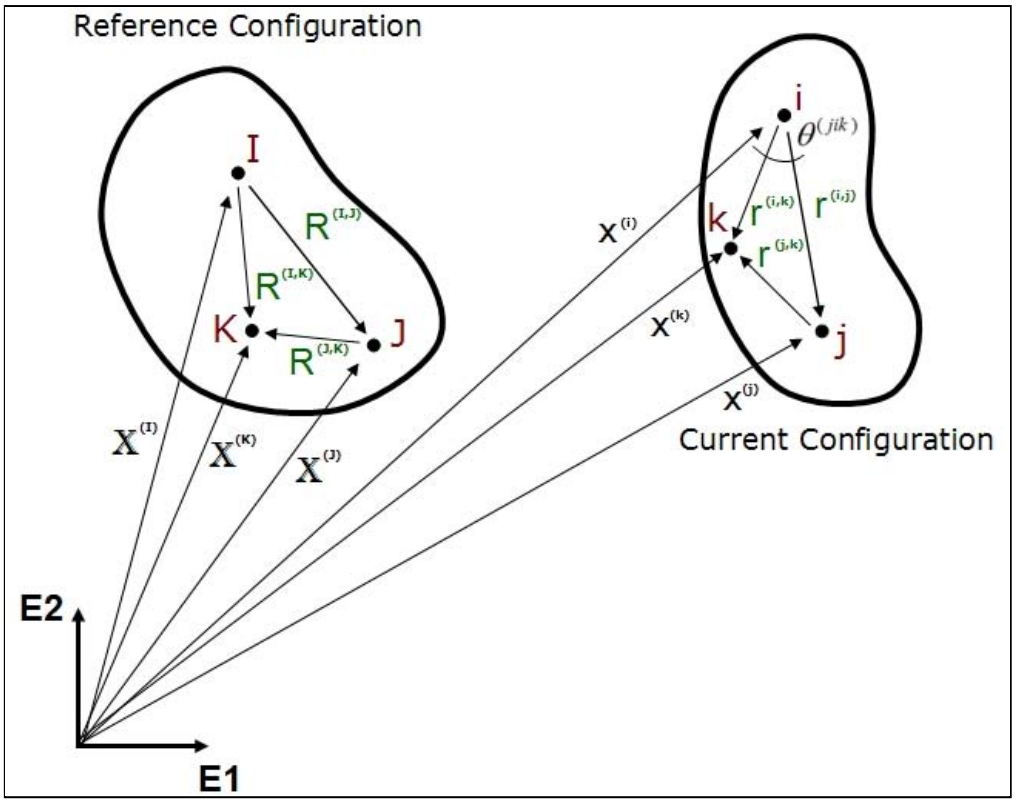

Figure 6. Three atoms depicted in the reference and current configurations.

In this report, the term “fine scale” refers to events occurring at atomistic scales on the order of 10 Angstroms, while the term “macroscale” refers to events occurring at scales larger than 100 μm (i.e., visible to the naked eye). The term “coarse scale” has a meaning synonymous with macroscale.

4. Atomistic Behavior and the Constitutive Equation

In formulating mathematical equations to model the physical world, material properties are incorporated via constitutive equations. The classical constitutive equation used in solid mechanics on the macroscale is Hooke’s law, and the tensor variable possessing the material behavior is the elasticity tensor denoted C_{IJKL}. Hooke’s law is stated as follows:

$$S_{IJ} = C_{IJKL} E_{KL}, \tag{1}$$

where S_{IJ} is the stress tensor and E_{KL} the strain tensor. In a loose sense, S_{IJ} embodies the forces acting on a body while E_{KL} embodies the displacements that occur as a result of these forces. It is a reasonable assumption, therefore, that if material behavior normally associated with the PZT fine scale is to be mathematically embedded into equations describing the macroscale, the elasticity tensor seen in Hooke’s law is where the embedding should occur. The formulation of an elasticity tensor encapsulating PZT atomistic behavior is needed for research.

5. Atomistic Elasticity Tensor

5.1 Atomistic Kinematics

Figure 6 depicts three atoms (i, j, and k) in the reference and current configurations. These atoms are located by Cartesian position vectors $\mathbf{X}^{(IJ)}, \mathbf{X}^{(IK)}, \mathbf{X}^{(JK)}$ and $\mathbf{x}^{(ij)}, \mathbf{x}^{(ik)}$, and $\mathbf{x}^{(jk)}$ in the reference and current configurations, respectively. The atoms may locally be described by their proximity to each other by the position vectors $\mathbf{R}^{(IJ)}, \mathbf{R}^{(IK)}, \mathbf{R}^{(JK)}$ and $\mathbf{r}^{(ij)}$, $\mathbf{r}^{(ik)}$, and $\mathbf{r}^{(jk)}$, also shown in respective configurations.

The angle created by two vectors subtending atom *i* is defined by the symbol $\theta^{(jik)} = \theta^{(kij)}$, where the atom subtended is the middle index. The cosine of this angle is therefore as follows:

$$\cos\theta^{(jik)} = \frac{\mathbf{r}^{(ij)}}{\left|\mathbf{r}^{(ij)}\right|} \cdot \frac{\mathbf{r}^{(ik)}}{\left|\mathbf{r}^{(ik)}\right|} = \frac{\mathbf{r}^{(ij)}}{r^{(ij)}} \cdot \frac{\mathbf{r}^{(ik)}}{r^{(ik)}}, \tag{2}$$

and

$$r^{(ij)} = \sqrt{\mathbf{r}^{(ij)} \cdot \mathbf{r}^{(ij)}}\ . \tag{3}$$

We note that all kinematic variables defined for any three atoms can be simplified to two vectors. For example, $\theta^{(jik)} = \theta^{(jik)}(\mathbf{r}^{(ij)}, \mathbf{r}^{(ik)})$ and $\mathbf{r}^{(jk)} = \mathbf{r}^{(ik)} - \mathbf{r}^{(ij)}$. Therefore, in what follows, the two truly independent variables are $\mathbf{r}^{(ij)}$ and $\mathbf{r}^{(ik)}$.

5.2 Definition of Potential

The form of the potential is given as follows:

$$\phi = \sum_{\substack{i,j \\ i<j}} v_2(i,j) + \sum_{\substack{i,j,k \\ i<j<k}} v_3(i,j,k), \tag{4}$$

where the first summation denotes pair interactions and the second summation the interactions of atom triples. Note that there is no factor of 1/2 contained in the equation because the summation conditions disallow double counting. The pair and triple terms are defined as follows:

$$v_2(i,j) = \varepsilon f_2(\mathrm{r}^{(ij)}/\sigma), \tag{5}$$

and

$$v_3(i,j,k) = \varepsilon f_3(\mathrm{r}^{(ij)}/\sigma, \mathrm{r}^{(ik)}/\sigma, \mathrm{r}^{(jk)}/\sigma), \tag{6}$$

where the constant ε is chosen to give the minimum of f_2 at –1, and σ is chosen to make $f_2(2^{1/6})$ vanish. These constants are given for Si in (Stillinger and Weber, 1985).

The pair term is a function of the scalar distance between two atoms, *i* and *j*, and is defined as follows:

$$f_2(r) = \begin{cases} A(Br^{-p} - r^{-q})\exp[(r-a)^{-1}], & r < a \\ 0, & r \geq a \end{cases}, \tag{7}$$

where *A, B, p, q,* and *a* are constants. The range of the pair interactions is limited to a circular region of radius *a* around each atom. The triple interaction is defined as follows:

$$f_3(\mathbf{r}^{(ij)}, \mathbf{r}^{(ik)}, \mathbf{r}^{(jk)}) = h(r^{(ij)}, r^{(ik)}, \theta^{(jik)}) + h(r^{(ji)}, r^{(jk)}, \theta^{(ijk)}) + h(r^{(ki)}, r^{(kj)}, \theta^{(ikj)}), \tag{8}$$

where

$$h(r^{(ij)}, r^{(ik)}, \theta^{(jik)}) = \lambda \exp\left[\gamma\left(r^{(ij)} - a\right)^{-1} + \gamma\left(r^{(ik)} - a\right)^{-1}\right]\left[\cos\theta^{(jik)} + \tfrac{1}{3}\right]^2. \tag{9}$$

Based on the previous discussion that there are only two true independent variables, we can redefine *h* in the form of some functions $\bar{h}^{(i)}$ and $h^{(i)}$ so that equation 8 can be rewritten as follows:

$$\begin{aligned} f_3 &= \bar{h}^{(i)}(|\mathbf{r}^{(ij)}|, |\mathbf{r}^{(ik)}|) + \bar{h}^{(j)}(|\mathbf{r}^{(ji)}|, |\mathbf{r}^{(jk)}|) + \bar{h}^{(k)}(|\mathbf{r}^{(ki)}|, |\mathbf{r}^{(kj)}|) \\ &= h^{(i)}(\mathbf{r}^{(ij)}, \mathbf{r}^{(ik)}) + h^{(j)}(\mathbf{r}^{(ji)}, \mathbf{r}^{(jk)}) + h^{(k)}(\mathbf{r}^{(ki)}, \mathbf{r}^{(kj)}) \\ &= h^{(i)}(\mathbf{r}^{(ij)}, \mathbf{r}^{(ik)}) + h^{(j)}(-\mathbf{r}^{(ij)}, \mathbf{r}^{(ik)} - \mathbf{r}^{(ij)}) + h^{(k)}(-\mathbf{r}^{(ik)}, \mathbf{r}^{(ij)} - \mathbf{r}^{(ik)}), \end{aligned} \tag{10}$$

where

$$h^{(i)}(\mathbf{r}^{(ij)},\mathbf{r}^{(ik)}) = \lambda \exp\left[\gamma\left(\sqrt{\mathbf{r}^{(ij)}\cdot\mathbf{r}^{(ij)}}-a\right)^{-1}+\gamma\left(\sqrt{\mathbf{r}^{(ik)}\cdot\mathbf{r}^{(ik)}}-a\right)^{-1}\right]\left[\frac{\mathbf{r}^{(ij)}}{\left|\mathbf{r}^{(ij)}\right|}\cdot\frac{\mathbf{r}^{(ik)}}{\left|\mathbf{r}^{(ik)}\right|}+\tfrac{1}{3}\right]. \qquad (11)$$

5.3 Finite Strain and Classical Continuum Mechanics

The atoms labeled *i*, *j*, and *k* are assumed in the deformed configuration. The equations thus far are only considering the instantaneous configuration to evaluate the energies from equation 4. From a Lagrangian continuum solid mechanics perspective, it is important to know how those atoms got there. We therefore define atoms labeled *I*, *J*, and *K* as the reference configuration relative to the original Cartesian basis.

We consider only affine deformations, meaning that the deformation process at the atomic scale is assumed to work in the same way as the continuum scale. Under this one-to-one mapping assumption, position vectors in the reference configuration **R** get transformed to the current configuration **r** through the deformation tensor **F,**

$$(\mathbf{r})_i = (\mathbf{FR})_i = r_i = \sum_I F_{iI}R_I = F_{iI}R_I\,, \qquad (12)$$

where repeated indices are assumed summation.

We use the conventional strain measures for the Green strain and Right Cauchy-Green strain, respectively, as follows:

$$E_{IJ} = \tfrac{1}{2}(F_{iI}F_{iJ} - \delta_{IJ}), \qquad (13)$$

and

$$C_{IJ} = F_{iI}F_{iJ}\,. \qquad (14)$$

We can then obtain a host of elasticity tensors by taking second derivatives of a strain energy function. From equation 4, the strain energy function is defined by the following:

$$\Phi = \frac{1}{N}\left(\phi(r) - \phi(R)\right), \qquad (15)$$

where *N* is the number of atoms. Different types of elasticity tensors may then be determined. For example, we may choose among the following fourth-order tensors:

$$\frac{\partial^2\Phi}{\partial C_{IJ}\partial C_{KL}}, \frac{\partial^2\Phi}{\partial E_{IJ}\partial E_{KL}}, \frac{\partial^2\Phi}{\partial F_{iJ}\partial F_{kL}}, \frac{\partial^2\Phi}{\partial \varepsilon_{ij}\partial \varepsilon_{kl}}, \qquad (16)$$

where the last tensor is based on the infinitesimal strain and would give the standard infinitesimal elastic constants after taking appropriate directional derivatives.

The process for obtaining any of the elastic property tensors is identical. We make repeated use of the chain rule to analytically determine the derivatives. Let us consider the following elastic tensor as the illustrative example:

$$\mathbb{C}_{IJKL} = \frac{\partial^2 \Phi}{\partial C_{IJ} \partial C_{KL}}. \tag{17}$$

By making use of earlier definitions, we proceed as follows:

$$\begin{aligned}
\mathbb{C}_{IJKL} &= \frac{\partial^2 \Phi}{\partial C_{IJ} \partial C_{KL}} \\
&= \frac{\partial^2 \Phi}{\partial F_{mN} \partial F_{pQ}} \frac{\partial F_{mN}}{\partial C_{IJ}} \frac{\partial F_{pQ}}{\partial C_{KL}} \\
&= \left(\begin{array}{l} \dfrac{\partial^2 \Phi}{\partial r_i^{(ij)} \partial r_j^{(ik)}} \dfrac{\partial r_i^{(ij)}}{\partial F_{mN}} \dfrac{\partial r_j^{(ik)}}{\partial F_{pQ}} + \dfrac{\partial^2 \Phi}{\partial r_i^{(ij)} \partial r_j^{(ij)}} \dfrac{\partial r_i^{(ij)}}{\partial F_{mN}} \dfrac{\partial r_j^{(ij)}}{\partial F_{pQ}} \\ \quad + \dfrac{\partial^2 \Phi}{\partial r_i^{(ik)} \partial r_j^{(ik)}} \dfrac{\partial r_i^{(ik)}}{\partial F_{mN}} \dfrac{\partial r_j^{(ik)}}{\partial F_{pQ}} + \dfrac{\partial^2 \Phi}{\partial r_i^{(ik)} \partial r_j^{(ij)}} \dfrac{\partial r_i^{(ik)}}{\partial F_{mN}} \dfrac{\partial r_j^{(ij)}}{\partial F_{pQ}} \end{array} \right) \frac{\partial F_{mN}}{\partial C_{IJ}} \frac{\partial F_{pQ}}{\partial C_{KL}}.
\end{aligned} \tag{18}$$

It is important to recall that the summation convention does not apply to indices in parentheses. To complete the process of equation 18, we use the definition in equations 13 and 14 to obtain the following:

$$\frac{\partial F_{pQ}}{\partial C_{KL}} = \left(\frac{\partial C_{KL}}{\partial F_{pQ}} \right)^{-1} = \left(\frac{\partial (F_{iK} F_{iL})}{\partial F_{pQ}} \right)^{-1} = \left(F_{pL} \delta_{QK} + F_{pK} \delta_{QL} \right)^{-1}, \tag{19}$$

and equation 12 to obtain

$$\frac{\partial r_i^{(ij)}}{\partial F_{mN}} = \frac{\partial \left(F_{iI} R_I^{(ij)} \right)}{\partial F_{mN}} = \delta_{mi} \delta_{NI} R_I^{(ij)} = \delta_{mi} R_N^{(ij)}. \tag{20}$$

The only task that now remains is to evaluate the derivatives of the strain energy potential Φ with respect to the atomic vectors. This is also a straightforward procedure. We start with the first derivative as follows:

$$\frac{\partial \phi}{\partial r_p^{(ij)}} = \frac{\partial}{\partial r_p^{(ij)}} \left(\sum_{\substack{i,j \\ i<j}} v_2(i,j) + \sum_{\substack{i,j,k \\ i<j<k}} v_3(i,j,k) \right)$$

$$= \sum_{\substack{i,j \\ i<j}} \frac{\partial v_2}{\partial r_p^{(ij)}} + \sum_{\substack{i,j,k \\ i<j<k}} \frac{\partial v_3}{\partial r_p^{(ij)}}$$

$$= \sum_{\substack{i,j \\ i<j}} \varepsilon \frac{\partial f_2}{\partial r^{(ij)}} \frac{\partial r^{(ij)}}{\partial r_p^{(ij)}} + \sum_{\substack{i,j,k \\ i<j<k}} \varepsilon \left(\frac{\partial h^{(i)}}{\partial r_p^{(ij)}} + \frac{\partial h^{(j)}}{\partial r_p^{(ij)}} + \frac{\partial h^{(k)}}{\partial r_p^{(ij)}} \right), \tag{21}$$

where the derivative in the first term is given by the following:

$$\frac{\partial r^{(ij)}}{\partial r_p^{(ij)}} = \frac{\partial \sqrt{r_q^{(ij)} r_q^{(ij)}}}{\partial r_p^{(ij)}} = \frac{1}{2} \left(\sqrt{r_q^{(ij)} r_q^{(ij)}} \right)^{-1} \cdot 2 r_t^{(ij)} \delta_{tp} = \frac{r_p^{(ij)}}{r^{(ij)}}. \tag{22}$$

Note that $\partial r^{(ij)} / \partial r_p^{(ik)} = \partial r^{(ik)} / \partial r_p^{(ij)} = 0$. Also, the derivative of the nonzero part of f_2 is as follows:

$$\frac{\partial f_2}{\partial r} = A \exp[(r-a)^{-1}] \left[-B r^{-p} \left(\frac{p}{r} + \frac{1}{(a-r)^2} \right) + r^{-q} \left(\frac{q}{r} + \frac{1}{(a-r)^2} \right) \right]. \tag{23}$$

A similar derivative needs to be evaluated for $h^{(i)}$.

Likewise, the key second derivatives that need to be derived are as follows:

$$\frac{\partial^2 \phi}{\partial r_p^{(ij)} \partial r_q^{(ij)}}, \frac{\partial^2 \phi}{\partial r_p^{(ij)} \partial r_q^{(ik)}}, \frac{\partial^2 \phi}{\partial r_p^{(ik)} \partial r_q^{(ij)}}, \frac{\partial^2 \phi}{\partial r_p^{(ik)} \partial r_q^{(ik)}}, \tag{24}$$

which will contain expressions such as

$$\frac{\partial r^{(ij)}}{\partial r_p^{(ij)} \partial r_q^{(ij)}} = \frac{\partial \left(r_p^{(ij)} / r^{(ij)} \right)}{\partial r_q^{(ij)}} = \frac{1}{r^{(ij)}} \delta_{pq} + r_p^{(ij)} \frac{\partial \left(1 / r^{(ij)} \right)}{\partial r_q^{(ij)}} = \frac{1}{r^{(ij)}} \left(\delta_{pq} + \frac{r_p^{(ij)}}{r^{(ij)}} \frac{r_q^{(ij)}}{r^{(ij)}} \right). \tag{25}$$

By observing the equations thus far, the elastic stiffness tensor is fully determined. The remaining task is extensive symbolic manipulations to obtain a closed form expression (if so desired) of the tensor, with repeated use of partial derivatives and chain rule multiplications. Due to the algebraic complexity of the potential function, the final expression is generally lengthy, but still obtainable.

6. Variational Multiscale Formulation

While the elasticity tensor formulated in section 5 will confine the displacement of PZT atoms to proper paths and distances within the atomic lattice, a coupling between these atomic displacements and the electric field $\tilde{\mathbf{E}}$ is needed. Moreover, the governing equations for $\tilde{\mathbf{E}}$

(i.e., Maxwell's equations) must be present in the overarching mathematical model since they share a role equal to those of solid mechanics regarding piezoelectric phenomenon. To allow for this, the equations used in this model will be formulated in a variational multiscale framework.

6.1 Multiscale Deformation

In the variational multiscale context, the displacement $\mathbf{u}$ of any point in the body (assumed synonymous with an atom's displacement) is decomposed into two parts $\mathbf{u}^{\alpha}$ and $\mathbf{u}^{\beta}$, whereby $\mathbf{u}^{\alpha}$ is a local displacement on the fine-scale and $\mathbf{u}^{\beta}$ is a global displacement on the macroscale. Figure 7 shows a pictorial example of this notion.

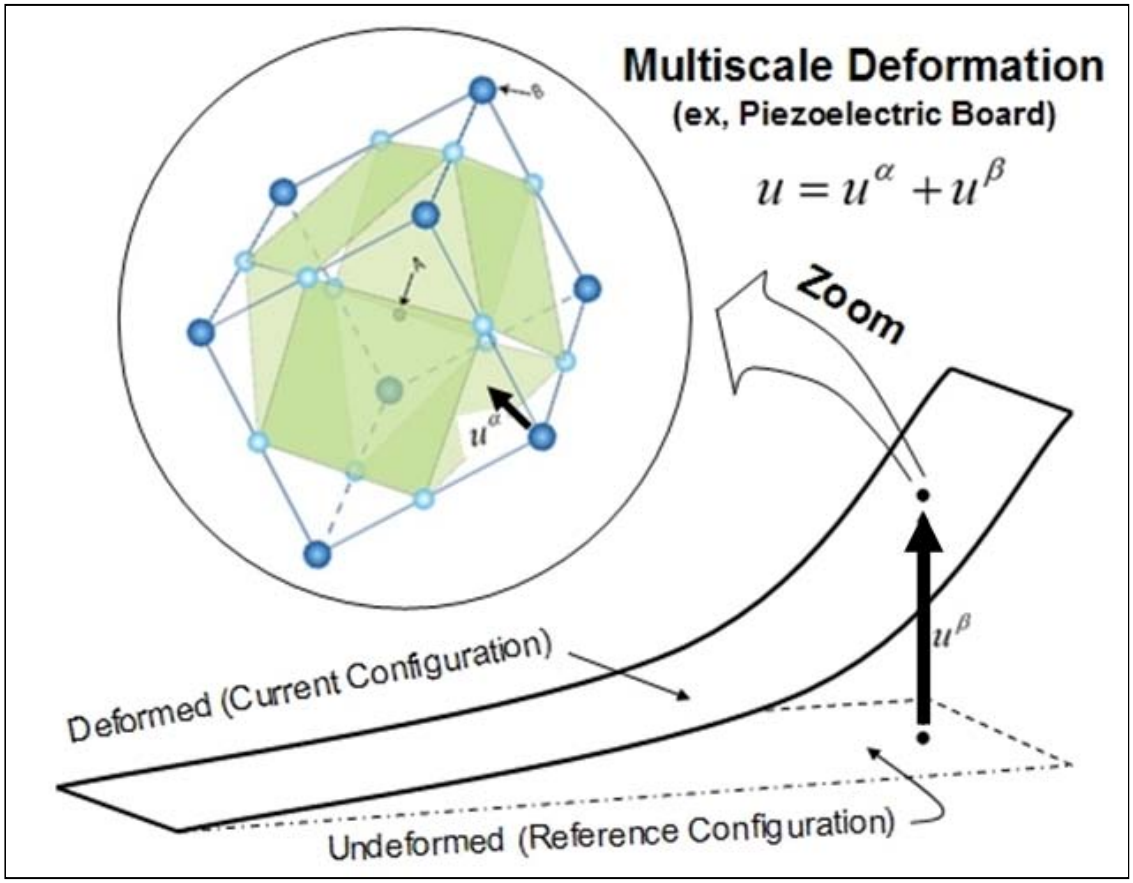

Figure 7. Example of multiscale deformation as seen by a piezoelectric board experiencing bending.

Figure 8 demonstrates some additional key points regarding variational multiscale deformation. In this figure, a hypothetically thin rod is used to demonstrate that (1) displacement $\mathbf{u}^{\alpha}$ will have a magnitude on the order of Angstroms, while $\mathbf{u}^{\beta}$ will have a magnitude on the order of meters; (2) strain is scale independent – a point that will be very important in subsequent sections; and (3) displacement $\mathbf{u}^{\beta}$ occurs due to the summation of a very large number of fine-scale displacements $\mathbf{u}^{\alpha}$ occurring over the entire body.

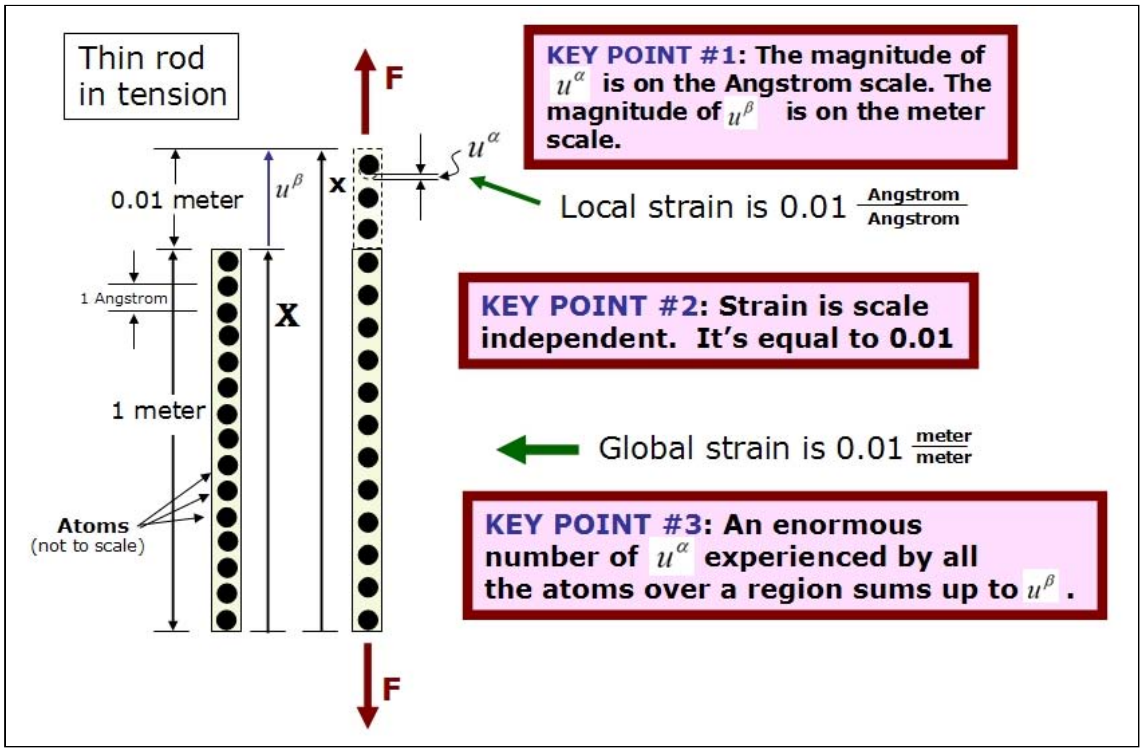

Figure 8. Some key points made by observing the deformations in a hypothetical thin wire.

6.2 Multiscale Kinematics

To accommodate fine-scale and coarse-scale equations, an additional intermediate configuration $\bar{\beta}$ is introduced to the two-configuration arrangement seen in classical continuum mechanics (see figure 6). The three configurations are shown in figure 9. In this figure, the position of a point in the intermediate configuration is denoted by $\overline{\mathbf{X}}$.

With these configurations, a logical definition of variables leads to simplistic equations. If displacements are defined as

$$\mathbf{u}^{\alpha} := \overline{\mathbf{X}} - \mathbf{X}, \tag{26}$$

$$\mathbf{u}^{\beta} := \mathbf{x} - \overline{\mathbf{X}}, \tag{27}$$

and

$$\mathbf{u} := \mathbf{x} - \mathbf{X}, \tag{28}$$

then, as desired, $\mathbf{u} = \mathbf{u}^{\alpha} + \mathbf{u}^{\beta}$. Defining the deformation gradients as

$$\mathbf{F} := \frac{\mathbf{dx}}{\mathbf{dX}}, \tag{29}$$

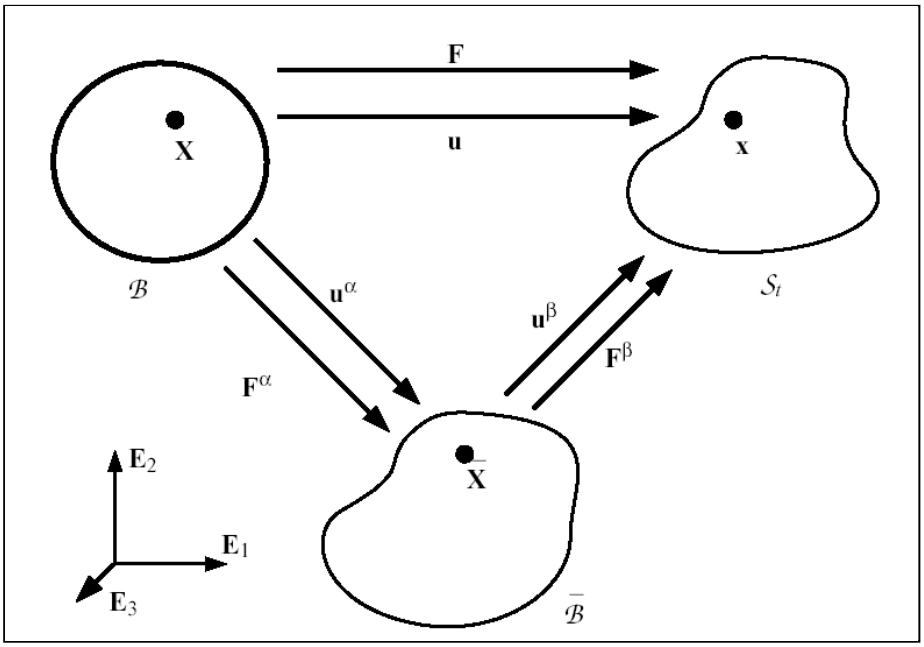

Figure 9. Multiscale kinematics. Three configurations are used in this framework – reference, intermediate, and current (Creighton et al., 2004).

$$\mathbf{F}^{\beta} := \frac{\mathbf{dx}}{\mathbf{d\bar{X}}}, \tag{30}$$

and

$$\mathbf{F}^{\alpha} := \frac{\mathbf{d\bar{X}}}{\mathbf{dX}} \tag{31}$$

yields the following equations:

$$\mathbf{F} = \mathbf{F}^{\beta}\mathbf{F}^{\alpha}, \tag{32}$$

$$\mathbf{F}^{\alpha} = \mathbf{I} + \frac{\partial \mathbf{u}^{\alpha}}{\partial \mathbf{X}}, \tag{33}$$

and

$$\mathbf{F}^{\beta} = \mathbf{I} - \nabla \mathbf{u}^{\beta}, \tag{34}$$

where the nabla symbol represents derivatives taken with respect the current position vector $\mathbf{x}$ such that $\nabla(\bullet) := \frac{\partial(\bullet)}{\partial \mathbf{x}}$. From these equations, we define the multiscale Green tensor as

$$\mathbf{E}^{\beta} := \frac{\mathbf{1}}{\mathbf{2}}\left(\mathbf{F}^{\beta^{\mathrm{T}}}\mathbf{F}^{\beta} + \mathbf{1}\right) \tag{35}$$

and the multiscale Right Cauchy-Green tensor as

$$\mathbf{C}^{\beta} := \mathbf{F}^{\beta^T}\mathbf{F}^{\beta}. \tag{36}$$

For a rigorous derivation of the variables, see Creighton et al. (2004).

6.3 Multiscale Governing Equations of Solid Mechanics

With the kinematic variables defined, we recall macroscale equations. Equations 37–39 are (1) the conservation of linear momentum, (2) a push forward of the second Piola-Kirchhoff stress tensor **S** to the current configuration, and (3) Hooke's law. Note the appropriateness of the β superscript in the following macroscale equations (recall that $\mathbf{u}^{\beta}$ is macroscale displacement):

$$\nabla \cdot \boldsymbol{\sigma} + \mathbf{b} = \rho\ddot{\mathbf{u}}^{\beta}, \tag{37}$$

$$\boldsymbol{\sigma} = \frac{1}{\mathbf{J}}\mathbf{F}^{\beta}\mathbf{S}\mathbf{F}^{\beta^T}, \tag{38}$$

and

$$\mathbf{S} = \mathbf{C} : \mathbf{E}^{\beta}. \tag{39}$$

Recalling equation 17 from section 5, the multiscale version of this equation becomes

$$\mathbf{C} = \frac{\partial^2 \boldsymbol{\Phi}}{\partial \mathbf{C}^{\beta} \partial \mathbf{C}^{\beta}}. \tag{40}$$

It should be noted that using $\mathbf{C}^{\beta}$ in the derivation of the atomistic elasticity tensor $\mathbf{C}$ is appropriate since strains are scale independent (see key point no. 2 in figure 8). Conversely, incorporating the macroscale displacement variable $\mathbf{u}^{\beta}$ into the formulation of $\mathbf{C}$ would be inappropriate due to its scale.

6.4 Governing Equations of Electromagnetism

The governing equations for electromagnetism are Maxwell's equations. From these equations, a relationship for the electric field vector $\tilde{\tilde{\mathbf{E}}}$ can be written as follows:

$$\frac{1}{\mu}\nabla \times \nabla \times \tilde{\tilde{\mathbf{E}}} + \varepsilon\ddot{\tilde{\tilde{\mathbf{E}}}} + \gamma\dot{\tilde{\tilde{\mathbf{E}}}} = \mathbf{0}. \tag{41}$$

(See Weidlinger Associates Inc. [1991] for the derivation.) Recognizing that the force exerted on a particle (or atom) of charge q_o in an electric field is

$$\mathbf{F} = q_o\tilde{\tilde{\mathbf{E}}} \tag{42}$$

and that Newton's Second Law for the atom is

$$\mathbf{F} = m\ddot{\mathbf{u}}^{\alpha}, \tag{43}$$

these two equations can be combined to create the following:

$$m\ddot{\vec{\mathbf{u}}}^{\alpha} = q_o \tilde{\mathbf{E}}, \tag{44}$$

or, alternatively,

$$\ddot{\vec{\mathbf{u}}}^{\alpha} = \tilde{q}\tilde{\mathbf{E}}, \tag{45}$$

where $\tilde{q} = \frac{q_o}{m}$ and m = $\frac{\left(0.48 \cdot mass(T_i) + 0.52 \cdot mass(Zr)\right)}{2}$ for the PZT at hand.

Consequently, equations 37, 41, and 45 constitute three equations and three unknowns which adequately describe the problem.

6.5 Variational Equations

Casting equations 37, 41, and 45 into the weak form for a numerical solution by the finite-element method, the problem is expressed mathematically as follows:

$$\mathcal{G}_1 := \int_{S_t} \nabla \mathbf{w}^{\beta} : \boldsymbol{\sigma}(\mathbf{u}^{\alpha}, \mathbf{u}^{\beta}) dS_t - \int_{S_t} (\mathbf{w}^{\beta} \cdot \mathbf{b}) dS_t - \int_{\partial S_t} (\mathbf{w}^{\beta} \cdot \mathbf{t}) d\partial S_t - \int_{S_t} (\mathbf{w}^{\beta} \cdot \rho \ddot{\mathbf{u}}^{\beta}) dS_t = \mathbf{0} \tag{46}$$

with unknowns $\{\mathbf{u}^{\alpha}, \mathbf{u}^{\beta}\}$.

$$\mathcal{G}_2 := \int_{S_t} \mathbf{w}^{\alpha} \cdot (\rho \ddot{\mathbf{u}}^{\alpha} - \tilde{q}\tilde{\mathbf{E}}) dS_t = \mathbf{0} \tag{47}$$

with unknowns $\{\mathbf{u}^{\alpha}, \tilde{\mathbf{E}}\}$.

$$\mathcal{G}_3 := \int_{S_t} \mathbf{w}^{E} \cdot \left(\frac{1}{\mu} \nabla \times \nabla \times \tilde{\mathbf{E}} \right) dS_t + \int_{S_t} \mathbf{w}^{E} \cdot \left(\varepsilon \ddot{\tilde{\mathbf{E}}} + \gamma \dot{\tilde{\mathbf{E}}} \right) dS_t = \mathbf{0} \tag{48}$$

with unknown $\{\tilde{\mathbf{E}}\}$.

---

7. Conclusions and Future Work

7.1 Atomistic Elasticity Tensor

The elastic property tensor will be a $3 \times 3 \times 3 \times 3$ fourth-order tensor which will have 81 nontrivial terms. All trivial/nontrivial terms and symmetries associated with the elastic tensor are determined solely by the crystal and NOT prescribed a priori. The challenge for the PZT structure at hand will be to capture the behavior of the different types of atoms (which vary significantly) when formulating the elasticity tensor $\mathbf{C}$. Moreover, using the potential in equation 9 is meant merely as an illustrative example of the procedure since it neglects long-range interactions common in piezoelectric materials.

7.2 Multiscale Formulation

Although the equations are all valid, issues concerning stability have not been addressed and will not be apparent until the stated weak form equations have been implemented and tested. Boundary conditions for $\mathbf{u}^{\alpha}$ and $\mathbf{u}^{\beta}$ also need to be addressed but can be modeled from earlier work in the field. An initial approach might be to use periodic boundary conditions for $\mathbf{u}^{\alpha}$ (used in most fine-scale molecular dynamics simulations), and boundary conditions typical of classic macro-scale solid mechanics for $\mathbf{u}^{\beta}$.

8. References

Creighton, S. L.; Regueiro, R. A.; Garikipati, K.; Klein, P. A.; Marin, E. B.; Bammann, D. J. A Variational Multiscale Method to Incorporate Strain Gradients in a Phenomenological Plasticity Model. *Computer Methods in Applied Mechanics and Engineering* **2004**, *193*, 5453–5475.

Labo, M. A.; Moraniec, S. M.; Schoelles, D. J. Soldier Design Competition: Portable Power Generation System, Capstone Project, Department of Civil and Mechanical Engineering, United States Military Academy, West Point, NY, 2005.

Rabe, K. M. Think Locally, Act Globally. *Nature Materials* **2002**, *1*, 147–148.

Stillinger, F.; Weber, T. A. *Phys. Rev. B* **1985**, *31* (8), 5262.

Weidlinger Associates Inc. EMFlex Theory – Sections 1 and 2. http://www.wai.com/AppliedScience/Software/Emflex/Reports/emflextheory.pdf (accessed 1991).

NO. OF
COPIES ORGANIZATION

1 (PDF only) DEFENSE TECHNICAL INFORMATION CTR
DTIC OCA
8725 JOHN J KINGMAN RD
STE 0944
FORT BELVOIR VA 22060-6218

1 DIRECTOR
US ARMY RESEARCH LAB
IMNE ALC IMS
2800 POWDER MILL RD
ADELPHI MD 20783-1197

1 DIRECTOR
US ARMY RESEARCH LAB
AMSRD ARL CI OK TL
2800 POWDER MILL RD
ADELPHI MD 20783-1197

1 DIRECTOR
US ARMY RESEARCH LAB
AMSRD ARL CI OK PE
2800 POWDER MILL RD
ADELPHI MD 20783-1197

ABERDEEN PROVING GROUND

1 DIR USARL
AMSRD ARL CI OK TP (BLDG 4600)

NO. OF
COPIES ORGANIZATION

1 DIRECTOR
US ARMY RESEARCH LAB
AMSRD ARL CI
J GOWENS
2800 POWDER MILL RD
ADELPHI MD 20783-1197

ABERDEEN PROVING GROUND

4 DIR USARL
AMSRD ARL CI HC
J CLARKE
AMSRD ARL WM M
J SMITH
AMSRD ARL WM TD
T BJERKE
AMSRD ARL WM TE
B RINGERS